Continuous synthesis of nanominerals in supercritical water

Marie Claverie, Marta Diez-garcia, François Martin, Cyril Aymonier

Continuous synthesis of nanominerals in supercritical water

Marie Claverie,[a] Marta Diez-Garcia,[b,c] François Martin,[d] Cyril Aymonier,*[c]

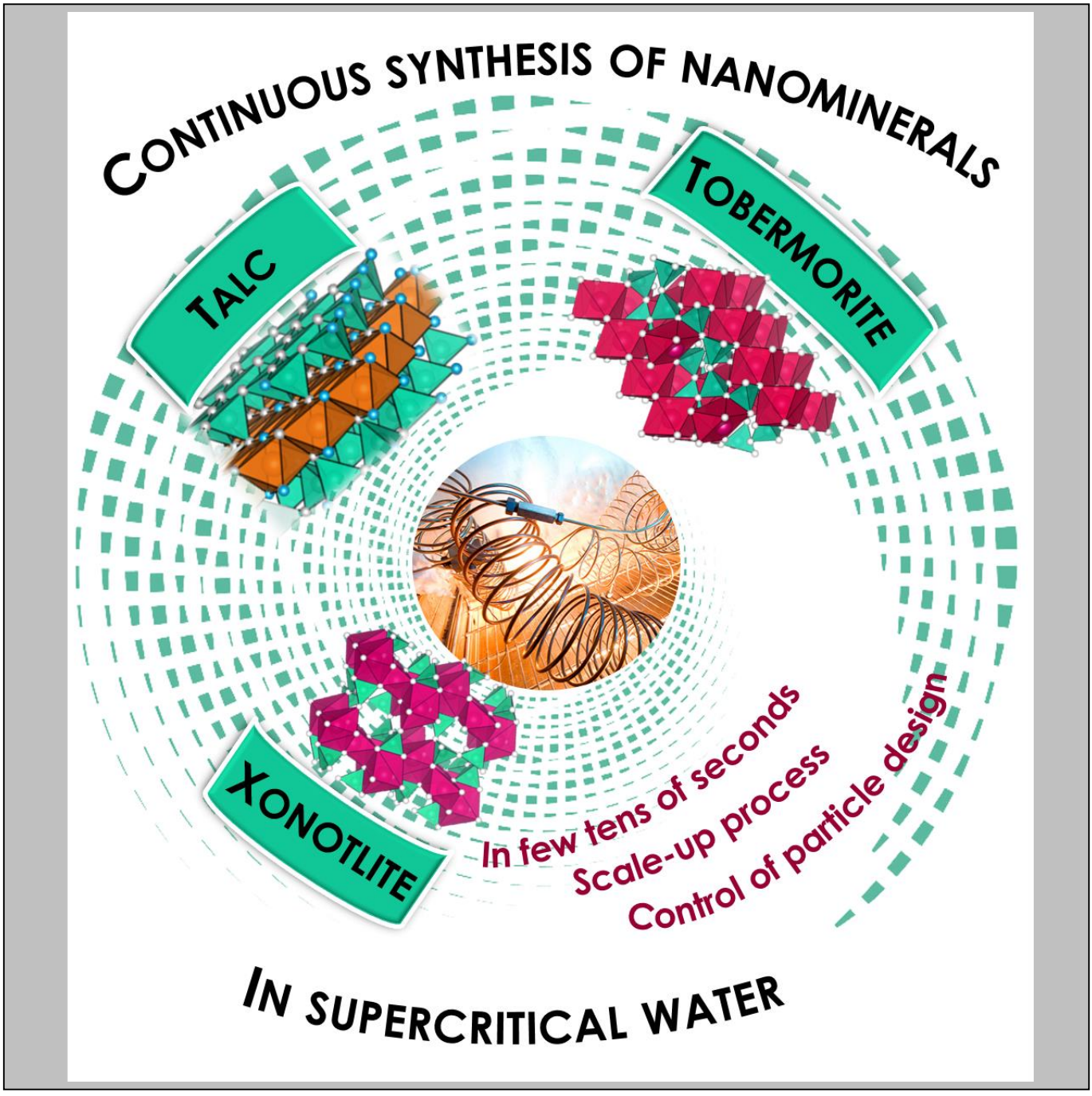

Abstract: The synthesis of minerals has to play a crucial role in the development of new and advanced materials. Since 2016, a renewal of interest to enlarge the mineral synthesis towards industrial requirements is observed, especially thanks to three main recent papers. The innovative process exposed combines a continuous process with the use of supercritical water. In addition to curtail synthesis times, this process offers a control on the particle characteristics (size, crystallinity, structure…) and a capacity to be easily transferable at an industrial scale. This innovative concept is demonstrated with the synthesis of three minerals which are the talc (a phyllomineral), the xonotlite and the tobermorite (two inominerals). This paper proposes an overview of the possibilities to synthesize nanominerals in continuous for the development of advanced materials with promising industrial applications.

1. Introduction

Minerals, consistently developed by inorganic processes (volcanic eruption, weathering of pre-existing minerals, precipitation by geological fluids), are defined as homogeneous solid including a specific chemical composition and a highly ordered atomic arrangement.[1] Minerals are formed in all geologic environments and thus under a wide range of chemical and physical conditions, such as varying temperature and pressure.[2] More than 5230 mineral species, identified by the International Mineralogical Association in March 2017, can be found worldwide.[3]

Since the middle of the 19th century, minerals are classified according to their chemical composition and more precisely, according to their dominant anion (sulfides, halides, carbonates…).[4,5] The silicates, major component of the earth's crust, represent the most significant mineral class. The fundamental unit of silicates is constituted of silicon-oxygen $(SiO_4)^{4-}$ tetrahedra. Due to their great variability in tetrahedra polymerization, silicates are themselves classified in six groups such as orthosilicates (isolated tetrahedra), inosilicates (chains and ribbons of tetrahedra) or phyllosilicates (sheets of tetrahedra) as many other.

Used to answer fundamental geological questions, minerals represent elemental and crucial raw materials in our daily life and are indispensable for economic, social and technological development.[6]

Attempt to imitate the most beautiful natural minerals is an ancient art: during the 1st century, Pliny the Elder already mentioned the manufacturing of stones to look like the most desired mineral.[4] It was not until the 19th century that the real synthesis of minerals known its first success. In 1847, Ebelmen synthesized several millimeter minerals such as emerald, corundum or spinel.[7] Nowadays, the number of technics to synthesize minerals is important and constantly improving. Synthetic minerals are generally purer than their natural counterparts (often associated with other minerals) in which the impurities damage properties for which they are used.

Knowledge of the methods in which natural minerals form and knowledge of the crystallography and crystal chemistry of natural minerals have helped scientists to synthesize a large variety of synthetic minerals. So, the synthetic mineral has so far been made by processes essentially similar to those which have operated on a much larger scale in nature. In this way, synthetic minerals can be obtained by:

- Cooling or evaporation of a saturated solution,
- Condensation of a vapor phase,
- Freezing of a liquid,
- Applying heat and pressure to a dry melt,
- Applying heat and pressure to a solid system containing water,
- Reactions involving ionic diffusion below the melting point.[4]

The general hydrothermal method extensively chosen to produce minerals makes use of a sealed container, bomb or autoclave.[4] It is supposed that conditions inside the enclosure resemble those that produced crystals in igneous rocks formerly subjected to high temperature and pressure. Nonetheless, this hydrothermal synthesis of mineral in a batch reactor is not easily transferrable at an industrial scale.

Synthetic minerals must comply with a nomenclature code dictated by The AIPEA Nomenclature Committee.[8,9] According to the nomenclature, a synthetic mineral should never be named ambiguously in order to distinguish it from the natural aspect of the mineral in question. The generic terms "phyllomineral" or "ino-mineral" are not considered by mineralogists in their natural state. Thus, we propose to use these designations to designate a phyllosilicate or inosilicate resulting from a synthesis.

One of the main objectives of this concept paper is to encompass an innovative continuous method to synthesize nanominerals in supercritical water. This new method presents the advantage to control chemistry and size and to be easily transferable at an industrial scale. This paper, after introducing the properties of

[a] M. Claverie
Imerys, 2 place Édouard Bouillières, 31100 Toulouse, France

[b] Dr. M. Diez-Garcia
Sustainable Construction Division, Tecnalia Parque tecnológico de Bizkaia, C/Geldo, Edif. 700, 48160, Derio (Spain)
UPV-EHU, Dep. Mining-Metallurgy Engeneering and Mat. Science, Alameda Urquijo s/n, 48013 Bilbao, Spain

[c] Dr. C. Aymonier, Dr. M. Diez-Garcia
CNRS, Univ. Bordeaux, Bordeaux INP, ICMCB, UMR 5026, F-33600 Pessac, France.
E-mail: cyril.aymonier@icmcb.cnrs.fr

[d] Prof . F. Martin
Geosciences Environnement Toulouse (GET), UMR 5563 UPS-CNRS-IRD-CNES, ERT 1074 Géomatériaux
14 Av. Edouard Belin, 31400 Toulouse (France)

supercritical water, enlightens the synthesis of three nanominerals which are: the talc, the xonotlite and the tobermorite.

2. Synthesis in supercritical water (SCW)

The supercritical fluid technology was widely exploited in applications such as extraction,[10,11] material synthesis,[12–16] water treatment [17], material recycling,[18] etc.

More precisely, supercritical water (SCW) has become significant as solvent for chemical reactions since the 1990s.[19] This rise of interest to use SCW appeared with intended purpose in the treatment of wastewater, in order to eliminate unbiodegradable substances.[20]

The pressure-temperature phase diagram of pure water is illustrated in Figure 1. For instance, the supercritical domain of water appears at temperatures higher than 374 °C and pressures over 22.1 MPa. It is possible to turn the properties of water on a wide scope just by adjusting the temperature and the pressure as shown in Figure 1 with the isochoric curves (dotted lines).

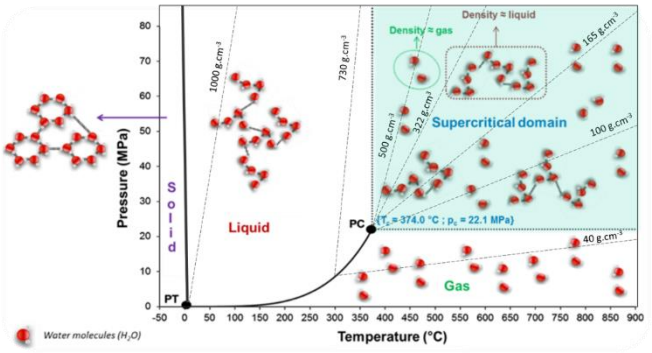

Figure 1. Pressure-temperature phase diagram of pure water. PT is the triple point (T_{PT} = 0 °C, P_{PT} = 0.612 MPa) and PC is the critical point (T_{PC} = 374 °C, P_{PC} = 22.1 MPa). Some isochoric curves are drawn (dotted lines). Reprinted with permission from ref [21].

In the supercritical domain, the physiochemical properties of water – density (ρ), dielectric constant (ε) and viscosity (η) – are intermediate between those of liquid and gas (Table 1). The water, for instance, highlights a drastic fall of its dielectric constant and density during the passage in the supercritical domain (Figure 2a). This phenomenon can be explained by the reduction of hydrogen bonds.[22,23] Moreover, the viscosity is reduced to gas-values in supercritical conditions, promoting the mass transfer. The non-dissociating nature of supercritical water is evidenced by the reduction by nine orders of magnitude of its ionic product (Figure 2b). All these properties allow the solubilization of non-polar compounds and the precipitation of inorganic compounds.[17] For this reason, it is possible to replace organic solvents by supercritical water which reveals ecological and economic interests.[24]

Moreover, an acceleration of the reaction kinetics is currently observed in supercritical water. An understanding of this "booster" effect was introduced by Adschiri *et al.* (in the case of ceria) thanks to the theory of Born relating the enhancement of the reaction rate (k) with the dielectric constant (ε):

$$\ln k = \ln k_0 - \frac{\omega}{RT}\left(\frac{1}{\varepsilon} - \frac{1}{\varepsilon_0}\right) \quad (1)$$

With ω a constant linked to the reaction system, k_0 the reaction rate at ε_0, T the absolute temperature and R the gas constant.[25]

Table 1. Physiochemical properties of water (liquid, subcritical, supercritical and superheated vapor).

	Liquid 25 °C 0.1 MPa	Subcritical Water 250 °C 5 MPa	Supercritical Water 400 °C 25 MPa	Overheated gas 400 °C 0.1 MPa
ρ (kg/m^3)	997	800	170	0.3
ε	78.5	27.1	5.9	1
η (μPa.s)	890	110	30	20

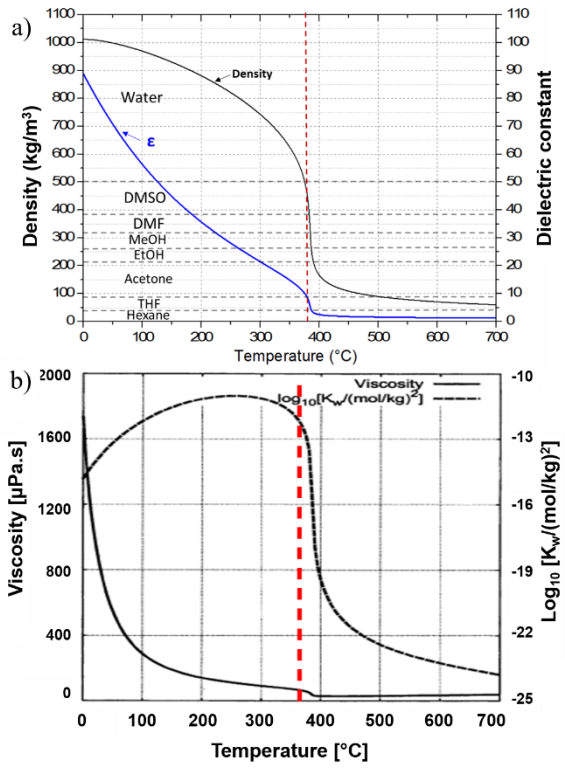

Figure 2. a) Evolution of density (ρ) and dielectric constant (ε) of water as a function of the temperature at 25 MPa. Comparison with common solvent values at room temperature and pressure. b) Evolution of viscosity and ionic product of water versus temperature at 25 MPa. Reprinted with permission from ref [17,26].

Recent reviews summarize the state-of-art of the continuous hydrothermal synthesis and applications of inorganic nanomaterials.[16,27,28] The authors highlight the decisive parameter to produce nanomaterials in a continuous supercritical hydrothermal process: the boost of supersaturation (ratio of the compound concentration in a solution to the saturation concentration). Indeed, this phenomenon intensifies the nucleation rate of particles leading to the formation of nanoparticles. It must be emphasized that these processes allow industrial scale applications. Generally, the use of supercritical water is part of an approach to sustainable development in which the use of toxic solvent must be overcome.[24]
More generally, another recent publication allows the better understanding of the synthesis of advanced inorganic nanomaterials using supercritical fluids.[16]

Currently, there are very few publications in the literature describing the environmental performance of supercritical fluids. Tsang *et al.* were the pioneers in this field with a publication of a study on the Life-Cycle Assessment (LCA) of the synthesis of barium strontium titanate in supercritical fluids.[29] Precursors (barium and titanium alkoxides) are the criterions with the highest environmental impact.
In another study recently published by the same authors, a LCA was published to compare the synthesis of 1 kg of TiO_2 by the supercritical route with a conventional precipitation method. The authors demonstrate a better performance for supercritical fluid synthesis.[30]
Finally, a third LCA study on the continuous hydrothermal or solvothermal synthesis of TiO_2 nanoparticles was also conducted.[31] These three publications highlight the interest of using supercritical fluids for the development of sustainable technologies, the precursor being the most important part of the environmental impact of the process.

A wide range of nanomaterials has been developed with the use of supercritical water that falls within bottom-up approaches.
In term of continuous process, the chemical reaction, nucleation and growth are implemented into a high temperature and high-pressure reactor and supplied with high-pressure pumps (Figure 3). The material synthesized can be recovered whether as a powder using a filter placed upstream the back-pressure regulator, or in suspension at the outlet of the process. This kind of set-up highlights an important flexibility. By varying the process operating parameters such as the pressure and temperature of the reactor, the nature and concentration of precursors and solvents and residence time within the reactor, it is so possible to control the inorganic (or inorganic/organic hybrid) nanoparticles design in terms of size, morphology, structure, crystallinity, composition and surface properties.[32–34]

In summary, the main interests of this process are:
- Ultra-fast reaction kinetics (tens of seconds): it is possible to operate in continuous mode leading to the possibility of a better control over the process,
- Ability to synthesize high quality nanoparticles in a single step,
- A process operating at a relatively low temperature (<400 °C) and using green solvents such as water,
- Scalability of this technology towards industrial production.

All these facts demonstrate that the supercritical water method reveals a sustainable and scalable way to synthesize high quality nanomaterials.

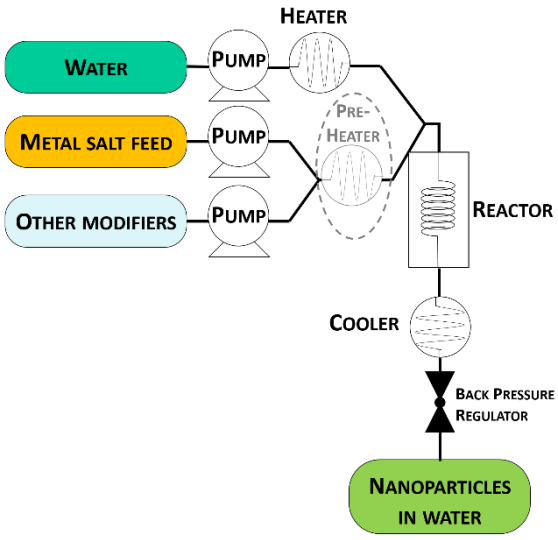

Figure 3. General chart of a continuous supercritical fluid process for nanomaterial synthesis.

3. Ultra-fast continuous synthesis of minerals in SCW

Herein we introduce pioneer works on the synthesis of three different nanominerals using a bottom-up approach with the supercritical hydrothermal flow synthesis.

3.1. The SCW continuous synthesis of talc

Talc is an integral part of daily life since it is currently used as mineral filler in paper, plastics, cosmetics, due to its lamellarity and chemical inertness (Figure 4).[35,36] Talc is a clay mineral composed of hydroxylated magnesium silicate with the chemical formula $Si_4Mg_3O_{10}(OH)_2$.[37]

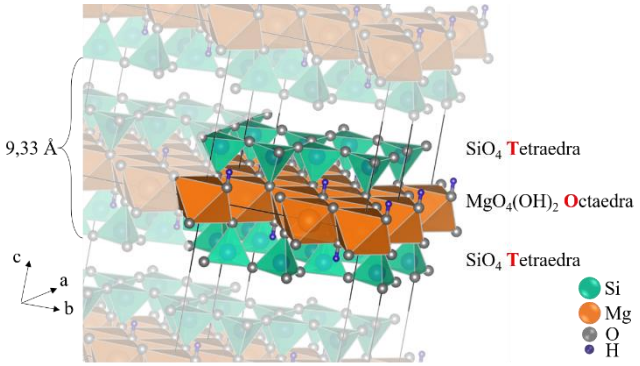

Figure 4. Crystal structure of talc (phyllosilicate) - 1 elementary layer = TOT + interlayer space. Reprinted with permission from ref [38].

Talc results from the transformation of preexistent magnesian or siliceous rocks by hydrothermal circulations. For instance, the talc deposit at Trimouns, in the French Pyrenees, derives from 14 million years of continuous circulation of hydrothermal fluids.[39] Conditions of genesis for this deposit are reckoned at 300-350 °C and 200-300 MPa.[40,41] However, natural talc suffers from some limitations in applications such as: 1) its association with other minerals (chlorite, carbonates, asbestos…), 2) its hydrophobic character and 3) its large micron-size (between 2 and 100 µm after industrial grinding). In this way, the talc synthesis brings a solution to obtain a mineral with a chemical purity and a particle size controlled. [42–45]

Since 1989, nanotalc can be synthesized in a batch reactor after a hydrothermal treatment.[38,46] Over the years, the synthesis protocol was revisited with the aim to reduce considerably the synthesis time from several days down to only few hours. By controlling the synthesis time, it is possible to control the particle size. This opportunity to finely tune particle-size was the origin of the nanotalc research and generated interest from industrials. This industrial interest was a driving-force to investigate new scalable synthesis method. One of the most interesting solution is the nanotalc synthesis in supercritical water. Dumas *et al.* enlightened the first talc synthesis combining a continuous set-up with the use of supercritical water.[47,48]

To perform the talc synthesis in only few tens of seconds, a mixture of silicon and magnesium in water, with a Si/Mg ratio equivalent to the Si/Mg talc ratio, is introduced in a reactor at 400 °C and 25 MPa.[48] During the synthesis, synthetic nanotalc is trapped in a filter as a gel form. A set of synthetic nanotalc was obtained in 10-23 seconds in near- or supercritical water.

This study reveals an ultra-fast structuration of synthetic nanotalc (Figure 5).[47] Synthetic nanotalc is a new material defined by a high chemical purity, a nano size (Figure 6) and a hydrophilic character.[47]

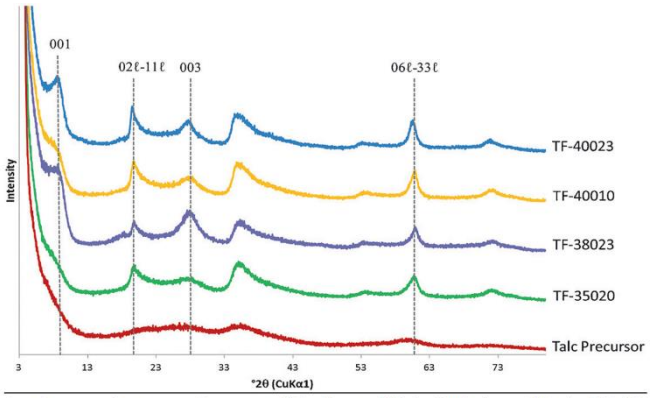

Sample	Reactor	Temperature [°C]	Pressure [MPa]	Synthesis duration [s]	CSD c* [Å]	CSD (ab) [Å]
TF-35020	Continuous	350	25	20–23	46 (1)	94 (2)
TF-38023		380			63 (1)	125 (4)
TF-40020		400			92 (3)	174 (8)
TF-40010				10	70 (2)	132 (5)
Talc precursor	Obtained at room temperature and ambient pressure				amorphous	

Figure 5. XRD patterns of nanotalc synthesized in supercritical water. The table lists the synthesis conditions and coherent scattering domain (CSD) measurements. Reprinted with permission from ref [47].

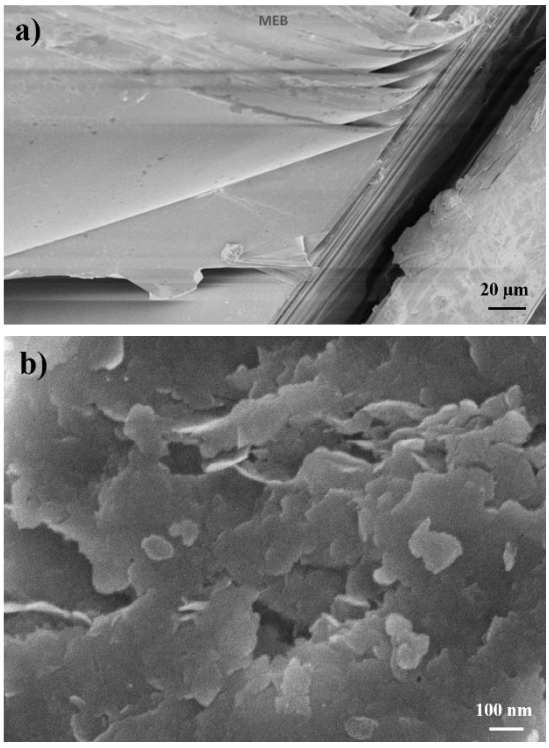

Figure 6. SEM images of a) natural talc and b) synthetic nanotalc (TF-40020) synthesized in supercritical water. Reprinted with permission from ref [45,47].

Figure 7 illustrates the crystal size coherency (estimated from the Scherrer relation)[49] which indicates the number of stacked layers in the c* direction (estimated from the 001 and 003 reflections) or the expansion of particles in the (ab) plane (calculated from the

06ℓ-33ℓ reflection) flawless. These diagrams show a crystallinity of the product obtained in continuous at 400°C and at 470°C in 20 seconds comparable to a talc synthesized in batch at 300°C for 2 hours and 6 hours, respectively. These results demonstrate the "booster" effect of the supercritical domain on the crystallinity of talc particles.

With a batch synthesis (at 300 °C, 8.5 MPa), the crystal size coherency (CSC) raises linearly in both directions with synthesis time. However, the evolution of the CSC for a continuous synthesis (at 25 MPa, in 20 seconds) reveals a different trend. Indeed, we can observe an increase of the CSC with the synthesis temperature with a regime change when accessing the supercritical domain (at T > 374 °C). This phenomenon can be explained by combined effects. Dumas *et al.* explained that the synthetic talc precursor entities (formed at the mixer point, upstream the reactor) are already formed of 10Å-wide T-O-T arrangements.[50] So, due to its numerous hydroxyl groups, the synthetic talc precursor can easily form hydrogen bonds and polar interaction with water. In supercritical conditions, the drastic fall of the water density and dielectric constant restricts the solvation of particles and consequently favors the convergence and interlocking of synthetic talc precursors. Consequently, the supercritical domain favors the growth of particles of synthetic talc.

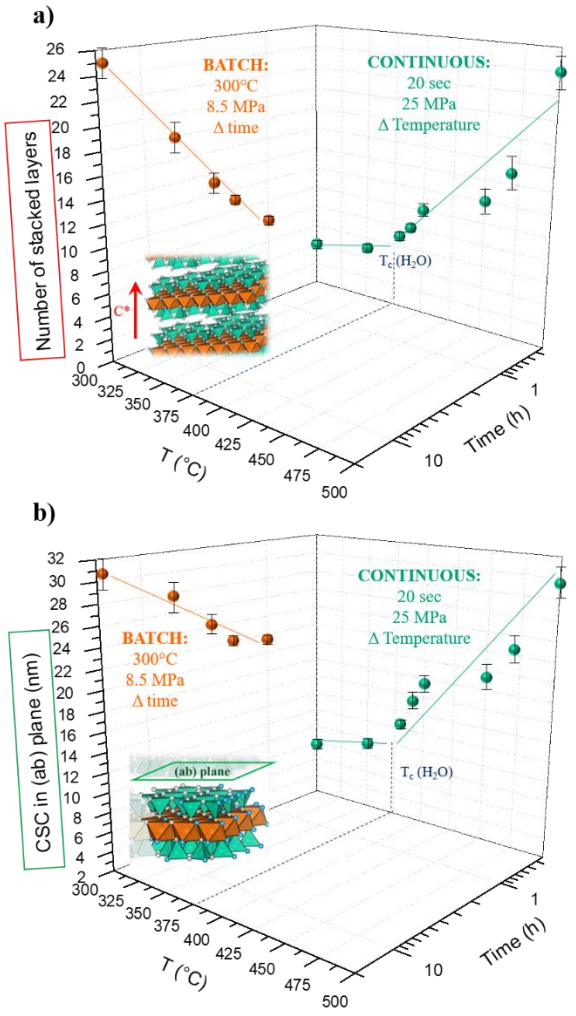

Figure 7. Evolution of crystal size coherency (CSC) in a) the c* direction (corresponding to the number of stacked layers) and b) the (ab) plane with synthesis time and temperature according to a continuous synthesis or a batch synthesis.

To conclude, this investigation reveals that it is possible to synthesize talc by using a continuous flow process and supercritical water. The supercritical domain is a key-parameter for the growth and structuration of particles in very curtail time. This new concept of talc synthesis makes it possible to reduce even more synthesis durations and can be a solution for the change of scale necessary for the industrialization.[38]

3.2. SCW for the synthesis of xonotlite

Xonotlite is a scarce calcium silicate hydrate mineral with formula $Ca_6Si_6O_{17}(OH)_2$. In nature, it is formed under hyper-alkali hydrothermal conditions.[51] In recent years the interest for this material has increased due to the potential applicabilities in several fields such as: additive for friction materials, precursor in

the synthesis of aerogels, for orthopedic applications and as addition for cement.[52–55]

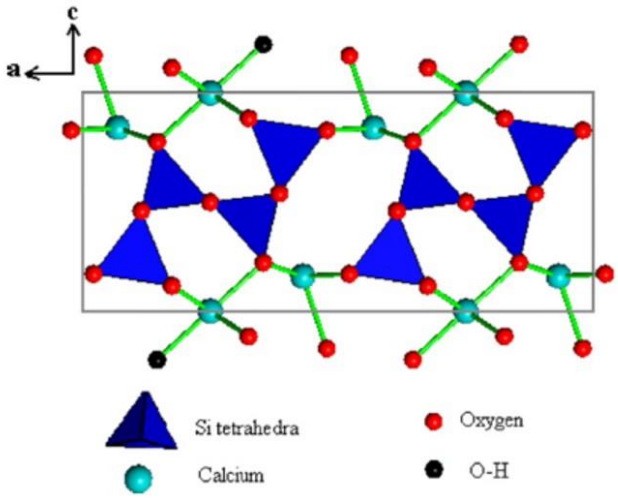

Figure 8. Structure of xonotlite. Reprinted with permission from ref [56].

The basic structure of xonotlite (Figure 8) is formed by wollastonite-like [Si_3O_9] chains, which consist of repetitive structures of 2n-1 SiO_4 tetrahedra where two of them are paired together, and the third one is in bonding position with the consecutive chain through the apical oxygen. The silicate chains are linked via undulating sheets of edge-sharing Ca polyhedra stacked along the c direction. The OH group is located at the free apices of the calcium octahedra where no SiO_4 tetrahedra are bonded.[57]

Xonotlite has traditionally been synthesized under mild hydrothermal conditions using as a precursor a suspension of silica and calcium oxide.[55,58,59] This process can last from 5 hours to 90 days depending on the conditions.[51,59] All the mentioned processes were carried out in a batch reactor. Recently Diez-Garcia *et al.* have developed a continuous process in supercritical water for the synthesis of xonotlite.[60] This study highlights the benefits of using supercritical water as a reaction media for the acquisition of highly crystalline synthetic xonotlite within few seconds of reaction, reducing the reaction time described for subcritical methods in several orders of magnitude.

For the synthesis stoichiometric amounts of $Na_2SiO_3 \cdot 9H_2O$ and $Ca(NO_3)_2 \cdot 4H_2O$ is injected into the reactor with a Ca/Si=1. An amorphous C-S-H gel precipitates as soon as both precursors are mixed, but the crystallization of the xonotlite takes place inside the tubular reactor at 400 °C and 25 MPa. The reaction occurs in just 20 seconds. The product obtained under supercritical conditions was compared to the one obtained under subcritical conditions at 300 ºC and 25 MPa for 20 seconds.[60] Under subcritical conditions, a poorly crystalized xonotlite is obtained. Under supercritical conditions, instead, highly crystalline and pure xonotlite is produced. These results are represented in the XRD analyses shown in Figure 9.

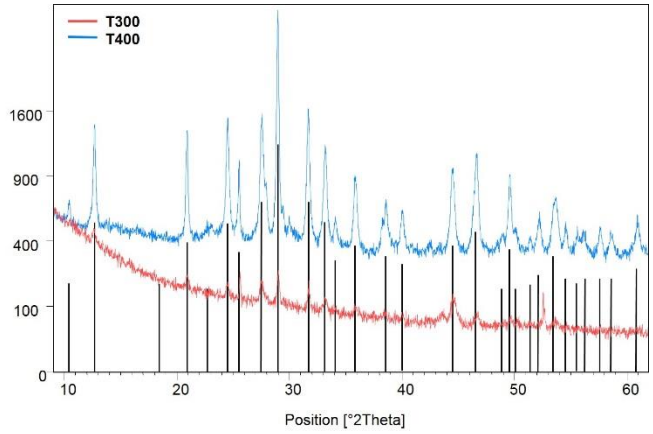

Figure 9. X-ray diffraction patterns of xonotlite synthesized at 300^{0}C and 400^{0}C compared with the reference (PDF 00-023-0125). Reprinted with permission from ref [60].

Figure 10 illustrates the morphology of the nanoparticles obtained under supercritical conditions. Synthetic xonotlite crystalized in the form of flat fibers of 1-10 µm long and 50-200 nm wide (Figure 10a). Through high-resolution TEM, it was possible to assess the preferential growing direction of the crystal. In Figure 9b, it is possible to observe two of the diffraction planes of the structure: the (200) and the (320). This information shows that the fibers grow along the direction of the silicate chains. Also, the preferential orientation in the plane (001), which is parallel to the grid, suggests that the thickness in the direction (001) is much smaller than the one in the (100) direction.

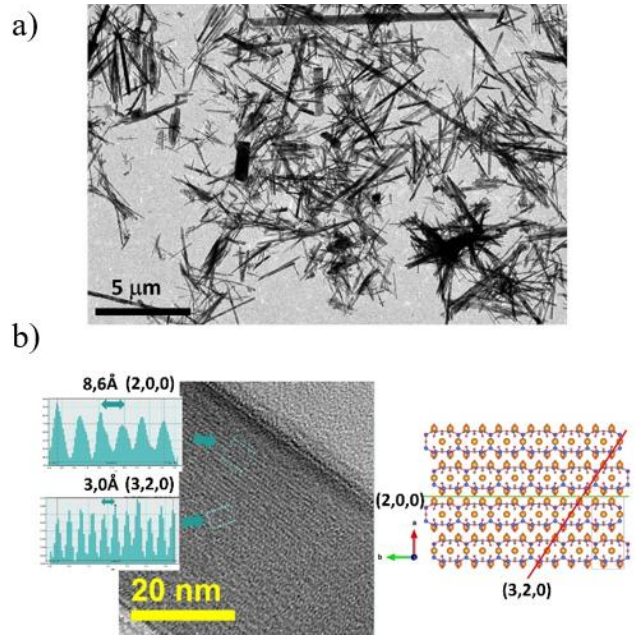

Figure 10. a) General TEM vision of the synthetic xonotlite nanofibers synthesized under supercritical conditions b) HR-TEM analysis of the synthetic xonotlite fibers and identification of two characteristic planes of the synthetic xonotlite structure. Reprinted with permission from ref [60].

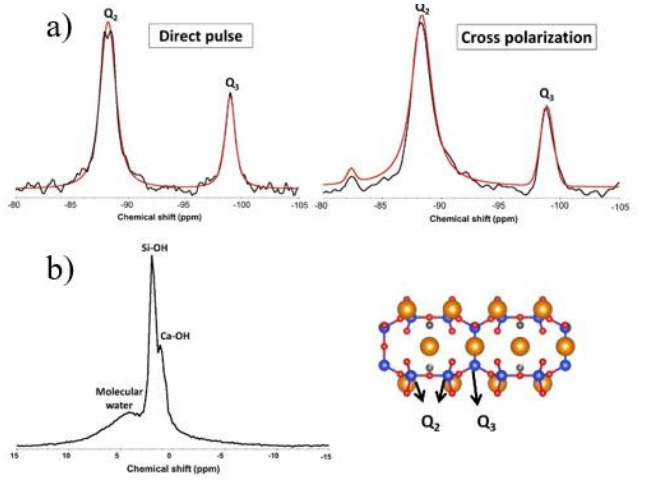

Figure 11. a) ^{29}Si MAS NMR spectra of synthetic xonotlite synthesized at 400^{0}C. Direct pulse (left) and cross-polarized (right) Black and red lines correspond to experimental and fitting results respectively. b) ^{1}H MAS NMR spectra of synthetic xonotlite. Reprinted with permission from ref [60].

The authors of this study also analyzed Si atom's environment through ^{29}Si MAS-NMR (Figure 11a). Two main signals are identified at -89 ppm and -99 ppm which correspond to Q_2 and Q_3 respectively (using common notation Q_n, where "n" represents the number of bridging oxygen sites per silicon tetrahedron "Q"). However, the authors observe a deviation from the ideal xonotlite structure. Whereas in the theoretical structure the Q_2:Q_3 areas ratio is 2:1, in the supercritical synthetic sample, this ratio is 2:0.7. Such discrepancy indicates that about 30% of the Q_3 Si sites are missing. The ^{1}H MAS-NMR experiments carried out by the authors (Figure 11b) proved the presence of Si-OH bonds in the synthetic xonotlite while in the ideal one only Ca-OH bonds should be present. Also, it was observed a difference of Q_2:Q_3 areas ratio among the ^{29}Si MAS-NMR carried out through direct pulse method, and the one carried out through cross polarization, being larger the area ratio in the first case. This observation confirms the proximity of H to Si atoms, more specifically to those in Q_2 positions.

Through these experiments, the authors claim that this anomaly is related to surface defects and propose that the surface of synthetic xonotlite might be formed by Si-OH groups, due to the lower solubility in water of SiO_2 compared to CaO. Through some crystallographic calculation, they prove the low thickness of the particles in the (001) direction (observed with TEM). This morphology gives, as a result, some surface defects that distort the Q_2:Q_3 areas ratio of these synthetic nanoparticles. In natural samples of xonotlite the crystal size is bigger, and these defects might be mitigated.

In conclusion, this work highlights the advantages of using the supercritical fluid technology to synthesize xonotlite. The product obtained is highly crystalline. Also, the reaction time employed for the synthesis has been reduced in several orders of magnitude compared with traditional hydrothermal subcritical synthesis. It has been demonstrated that, as a consequence of the nano-sized particles, some surface defects are observed. This new synthetic route opens new possibilities for the industrial use of this interesting mineral which is scarce in nature.

3.3. SCW for the synthesis of Tobermorite

Tobermorite is a calcium silicate hydrate in form of a fibrillar mineral with this chemical formula: $Ca_5Si_6O_{16}(OH)_2.nH_2O$. The importance of this compound resides in the fact that its structure is used as a model to explain the main phase of the cement paste, the C-S-H gel. Also, tobermorite is understood to be a key ingredient in the longevity of ancient undersea Roman concrete.[61,62] Nowadays, tobermorite has been proposed to be used as seeding addition for cement composites and as a stabilizing agent for the trap of impurities.[63–67]

Three structural varieties are distinguished, depending on the amount of water in the interlayer space: 14 Å tobermorite, 11 Å tobermorite (the most common structure under ambient conditions) or 9 Å tobermorite. The 11 Å tobermorite, referenced here as synthetic tobermorite (Figure 12), exists in two polymorphs: normal and anomalous. The difference between them is their behavior after the loss of water at 300 °C.[68] The normal polymorph will be transformed into 9 Å tobermorite while the anomalous one will remain stable. Due to its genesis in hyper-alkaline hydrothermal conditions, tobermorite is recognized as a

scarce mineral in nature.[51,69] This is the reason why tobermorite is synthesized to be industrially exploited.

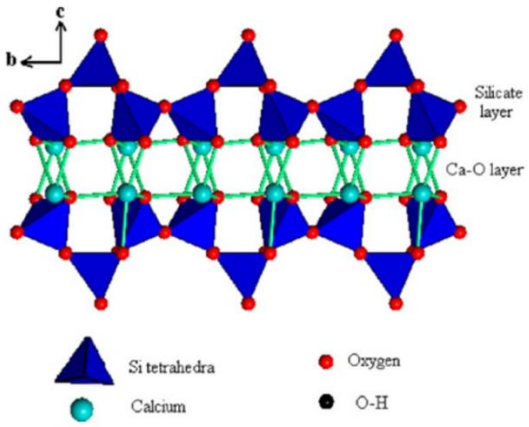

Figure 12. Structure of tobermorite. Reprinted with permission from ref [56].

The most common synthesis method involves a hydrothermal treatment in a batch reactor. Nevertheless, pure crystalline tobermorite is arduous to achieve being usually associated with amorphous or poorly ordered phase. Several studies were caried out to improve the crystallinity with the study of different parameters such as reaction duration, temperature, Ca/Si ratio, pH, precursor and partial substitution of silicon by aluminum.[67] Moreover, the effect of additives such as EDTA, sucrose, borosilicate or Ca-formate was also the subject of many studies. The hydrothermal process is usually performed at 200 °C during 5 hours to 56 days.[51,70–72] The temperature is a critical parameter since tobermorite is unstable (Ca/Si ratio not in the range of 0.8 to 1) under hydrothermal conditions and xonotlite starts to be formed at 130 °C.[67] Notwithstanding, many researches confirmed that partial substitution of silicon by aluminum increases the stability of tobermorite.[51,71,72]

Diez-Garcia *et al.* presents an innovative synthesis method which emphasizes again the use of supercritical water and a continuous flow reactor.[67] This study proposes the demonstration of the synthesis of a metastable phase under the synthesis conditions (synthetic tobermorite) thanks to the possibility to finely tune the reaction kinetics to counter the formation of the more thermodynamically stable material.

The synthesis is performed with the use of sodium metasilicate, calcium nitrate (Ca/(Si+Al) molar ratio of 0.83) and aluminum nitrate (Al/(Si+Al) molar ratio of 0.15) due to their high solubility in water. To prevent carbonation, these precursors are kept under N_2 flow during all the reaction and mixed to form an amorphous C-S-H gel in a T mixer piece placed upstream from the reactor. This gel is introduced in the reactor at 400 °C and 23.5 MPa where the crystallization occurs. A set of samples was obtained with different residence times (7, 10 and 15 seconds) and were compared with a synthetic tobermorite obtained after 4 hours of a conventional hydrothermal treatment (215 °C, endogenous pressure in a batch reactor) (Figure 13).

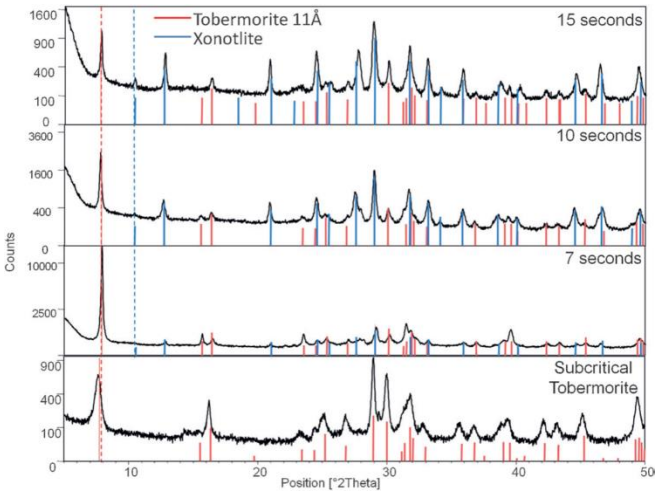

Figure 13. XRD patterns of synthetic tobermorite prepared in the continuous supercritical hydrothermal reactor (400 °C, 23.5 MPa) during 7, 10 or 15 seconds and compared with tobermorite synthesized with the conventional method (215 °C, 4h). Reprinted with permission from ref [67].

This research revealed that the most favorable residence time is 7 seconds. Tobermorite synthesized in supercritical water exhibits a fibrous form with a basal distance of 11 Å (Figure 14). The authors highlight a homogeneous nucleation process bringing to the formation of fibers with few tens of micrometers in length and few nanometers in width.[67] Due to a similar aspect to natural tobermorite, this synthesis method seems to be nearest to formation process that takes place in nature.

In conclusion, this method favors a greater regulation of synthesis time and conditions since it allows the crystallization of an unstable phase beyond its stability limit. Furthermore, due to an increase of reaction kinetics in supercritical conditions, synthesis times are reduced from several hours down to few seconds. Finally, tobermorite synthesized in supercritical conditions exhibits a morphology and structure close to the natural mineral suggesting that the supercritical process reproduces, in an accelerated basis, the geological genesis. In this sense, the supercritical hydrothermal process might provide a tool to fathom the geological processes that lead to the formation of phases under geothermal conditions.

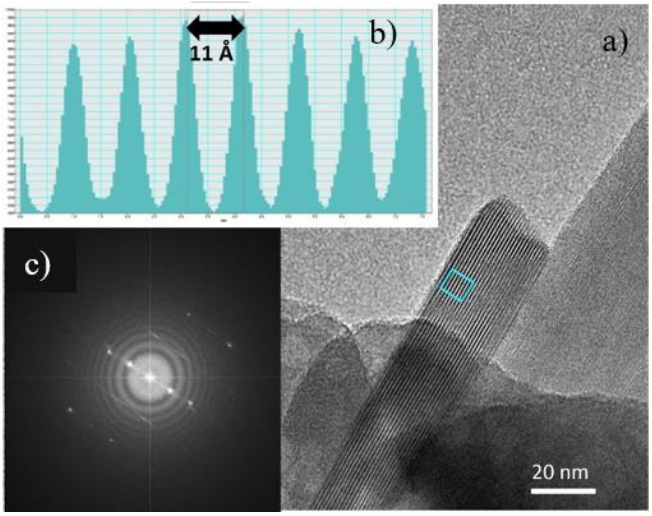

Figure 14. a) HR-TEM image of tobermorite synthesized in supercritical water. b) Profile extracted from the blue area in the a) and measure of the basal distance perpendicular to the fiber's axis. c) Fourier transform of this same area. Reprinted with permission from ref [67].

4. Conclusion

This concept article gives an overview of an innovative process to produce in continuous nanominerals. By the use of supercritical water, it is now possible to obtain a synthetic talc phyllomineral and two synthetic inominerals such as synthetic xonotlite and synthetic tobermorite in only few seconds and with the ability to be transferable at an industrial scale. This paper highlights the awareness attained from the synthesis of minerals which contributes to a greater insight of the geological genesis processes of natural minerals. This synthesis mechanism presents a direct approach to adjust the composition and properties, therefore offering a wide range of applications of the synthetic minerals. Synthetic minerals with well-controlled composition and structure offer advanced functional materials. In conclusion, the synthetic minerals are one of a prominent area in materials and the subject is of high relevance industrially and academically.

Keywords: continuous approach • hydrothermal synthesis • nanomineral • supercritical water • silicates •

[1] R. M. Hazen, J. H. Ausubel, *Am. Mineral.* **2016**, *101*, 1245–1251.
[2] R. L. Rudnick, S. Gao, *Treatise Geochem.* **2003**, *3*, 659.
[3] "International Mineralogical Association," can be found under https://www.ima-mineralogy.org/, **n.d.**
[4] F. Fouqué, A. Michel-Lévy, *Synthèse des minéraux et des roches*, G. Masson, Paris, **1882**.
[5] H.-R. Wenk, A. Bulakh, *Minerals: Their Constitution and Origin*, Cambridge University Press, **2004**.
[6] G. W. Josephson, *Ind. Eng. Chem.* **1955**, *47*, 426–431.
[7] J. J. Ebelmen, *Comptes Rendus Acad Sci Fr* **1844**, *19*, 398.
[8] E. H. Nickel, *Can. Mineral.* **1995**, *33*, 1335.
[9] S. Guggenheim, J. M. Adams, D. C. Bain, F. Bergaya, M. F. Brigatti, V. A. Drits, M. L. L. Formoso, E. Galán, T. Kogure, H. Stanjek, *Clays Clay Miner.* **2006**, *54*, 761–772.
[10] M. A. McHugh, V. J. Krukonis, *Supercritical Fluid Extraction: Principles and Practice.*, Butterworth-Heinemann, Boston, **1986**.
[11] H. Peker, M. P. Srinivasan, J. M. Smith, B. J. McCoy, *AIChE J.* **1992**, *38*, 761–770.
[12] C. Aymonier, A. Loppinet-Serani, H. Reverón, Y. Garrabos, F. Cansell, *J. Supercrit. Fluids* **2006**, *38*, 242–251.
[13] F. Cansell, C. Aymonier, A. Loppinet-Serani, *Curr. Opin. Solid State Mater. Sci.* **2003**, *7*, 331–340.
[14] D. Hojo, H. Ohara, T. Aida, G. Seong, N. Aoki, S. Takami, T. Adschiri, *J. Supercrit. Fluids* **2019**, *143*, 134–138.
[15] M. Türk, *Particle Formation with Supercritical Fluids Challenges and Limitations*, Elsevier, Amsterdam, **2014**.
[16] C. Aymonier, G. Philippot, A. Erriguible, S. Marre, *J. Supercrit. Fluids* **2018**, *134*, 184–196.
[17] T. Voisin, A. Erriguible, D. Ballenghien, D. Mateos, A. Kunegel, F. Cansell, C. Aymonier, *J. Supercrit. Fluids* **2017**, *120*, *Part 1*, 18–31.
[18] C. Morin, A. Loppinet-Serani, F. Cansell, C. Aymonier, *J. Supercrit. Fluids* **2012**, *66*, 232–240.
[19] T. Adschiri, K. Kanazawa, K. Arai, *J. Am. Ceram. Soc.* **1992**, *75*, 1019–1022.
[20] D. Bröll, C. Kaul, A. Krämer, P. Krammer, T. Richter, M. Jung, H. Vogel, P. Zehner, *Angew. Chem. Int. Ed Engl.* **1999**, *38*, 2998–3014.
[21] A. Loppinet-Serani, C. Aymonier, F. Cansell, *J. Chem. Technol. Biotechnol.* **2010**, *85*, 583–589.
[22] K. P. Johnston, C. Haynes, *AIChE J.* **1987**, *33*, 2017–2026.
[23] H. D. Cochran, P. T. Cummings, S. Karaborni, *Fluid Phase Equilibria* **1992**, *71*, 1–16.
[24] H. Machida, M. Takesue, R. L. Smith, *J. Supercrit. Fluids* **2011**, *60*, 2–15.
[25] T. Adschiri, Y. Hakuta, K. Arai, *Ind. Eng. Chem. Res.* **2000**, *39*, 4901–4907.
[26] M. Hodes, P. A. Marrone, G. T. Hong, K. A. Smith, J. W. Tester, *J. Supercrit. Fluids* **2004**, *29*, 265–288.
[27] J. A. Darr, J. Zhang, N. M. Makwana, X. Weng, *Chem. Rev.* **2017**, *117*, 11125–11238.
[28] T. Adschiri, A. Yoko, *J. Supercrit. Fluids* **2018**, *134*, 167–175.
[29] M. Tsang, G. Philippot, C. Aymonier, G. Sonnemann, *Green Chem.* **2016**, *18*, 4924–4933.
[30] M. Tsang, G. Philippot, C. Aymonier, G. Sonnemann, *ACS Sustain. Chem Eng* **2018**, *6*, 5142–5151.
[31] P. Caramazana-González, P. W. Dunne, M. Gimeno-Fabra, M. Zilka, M. Ticha, B. Stieberova, F. Freiberg, J. McKechnie, E. H. Lester, *Green Chem* **2017**, *19*, 1536–1547.
[32] H. Reverón, C. Aymonier, A. Loppinet-Serani, C. Elissalde, M. Maglione, F. Cansell, *Nanotechnology* **2005**, *16*, 1137–1143.
[33] R. Sui, P. Charpentier, *Chem. Rev.* **2012**, *112*, 3057–3082.
[34] G. Philippot, C. Elissalde, M. Maglione, C. Aymonier, *Adv. Powder Technol.* **2014**, *25*, 1415–1429.
[35] R. T. Martin, S. W. Bailey, D. D. Eberl, D. S. Fanning, S. Guggenheim, H. Kodama, D. R. Pevear, J. Srodon, F. J. Wicks, *Clays Clay Miner.* **1991**, *39*, 333–335.
[36] R. J. Haüy, *Traité de minéralogie*, Bachelier Et Huzard, **1822**.
[37] S. W. Bailey, *Clays Clay Miner.* **1969**, *17*, 355–371.
[38] M. Claverie, A. Dumas, C. Careme, M. Poirier, C. Le Roux, P. Micoud, F. Martin, C. Aymonier, *Chem. - Eur. J.* **2018**, *24*, 519–542.
[39] P. Boulvais, P. de Parseval, A. D'Hulst, P. Paris, *Mineral. Petrol.* **2006**, *88*, 499–526.
[40] U. Schärer, P. de Parseval, M. Polvé, M. de Saint Blanquat, *Terra Nova* **1999**, *11*, 30–37.
[41] P. de Parseval, S. Y. Jiang, F. Fontan, R. C. Wang, F. Martin, J. Freeet, *ResearchGate* **2004**, *20*, 877–886.

[42] L. F. Gate, *Preparation of Aqueous Suspensions of Talc*, **1984**, US4430249 (A).

[43] F. Martin, *Tech. Ing.* **2008**.

[44] F. Martin, E. Ferrage, S. Petit, P. de Parseval, L. Delmotte, J. Ferret, D. Arseguel, S. Salvi, *Eur. J. Mineral.* **2006**, 641–651.

[45] A. Dumas, F. Martin, C. L. Roux, P. Micoud, S. Petit, E. Ferrage, J. Brendlé, O. Grauby, M. Greenhill-Hooper, *Phys. Chem. Miner.* **2013**, *40*, 361–373.

[46] A. Dumas, F. Martin, E. Ferrage, P. Micoud, C. Le Roux, S. Petit, *Appl. Clay Sci.* **2013**, *85*, 8–18.

[47] A. Dumas, M. Claverie, C. Slostowski, G. Aubert, C. Careme, C. Le Roux, P. Micoud, F. Martin, C. Aymonier, *Angew. Chem. Int. Ed.* **2016**, *55*, 9868–9871.

[48] C. Aymonier, C. Slostowski, A. Dumas, P. Micoud, C. Le Roux, F. Martin, *(En) Process for the Continuous Preparation of Phyllomineral Synthetic Particles - WO 2015159006 A1 (Fr) Procédé De Préparation De Particules Synthétiques Phyllominérales En Continu - FR 3019813 A1*, **2015**, WO 2015159006 A1-FR 3019813 A1.

[49] G. Brown, P. Nadeau, *Philos. Trans. R. Soc. Lond. Ser. Math. Phys. Sci.* **1984**, *311*, 221–240.

[50] A. Dumas, M. Mizrahi, F. Martin, F. G. Requejo, *Cryst. Growth Des.* **2015**, *15*, 5451–5463.

[51] S. Shaw, S. M. Clark, C. M. B. Henderson, *Chem. Geol.* **2000**, *167*, 129–140.

[52] G. Wei, Y. Liu, X. Zhang, F. Yu, X. Du, *Int. J. Heat Mass Transf.* **2011**, *54*, 2355–2366.

[53] H. Traussnig, E. Kloimstein, H. Kroath, R. Estermann, *Extracting Agents for Poly-D(-)-3-Hydroxybutyric Acid*, **1990**, 4968611.

[54] X. Li, J. Chang, *J. Mater. Sci.* **2006**, *41*, 4944–4947.

[55] N. M. P. Low, J. J. Beaudoin, *Cem. Concr. Res.* **1993**, *23*, 1016–1028.

[56] N. Y. Mostafa, A. A. Shaltout, H. Omar, S. A. Abo-El-Enein, *J. Alloys Compd.* **2009**, *467*, 332–337.

[57] C. Hejny, T. Armbruster, *Z. Für Krist. - Cryst. Mater.* **2009**, *216*, 396–408.

[58] L. Black, K. Garbev, A. Stumm, *Adv. Appl. Ceram.* **2009**, *108*, 137–144.

[59] S.-Y. Hong, F. P. Glasser, *Cem. Concr. Res.* **2004**, *34*, 1529–1534.

[60] M. Diez-Garcia, J. J. Gaitero, J. I. Santos, J. S. Dolado, C. Aymonier, *J. Flow Chem.* **2018**, *8*, 89–95.

[61] M. D. Jackson, E. N. Landis, P. F. Brune, M. Vitti, H. Chen, Q. Li, M. Kunz, H.-R. Wenk, P. J. M. Monteiro, A. R. Ingraffea, *Proc. Natl. Acad. Sci. U. S. A.* **2014**, *111*, 18484–18489.

[62] T. Mitsuda, K. Sasaki, H. Ishida, *J. Am. Ceram. Soc.* **1992**, *75*, 1858–1863.

[63] U. Berg, D. Donnert, P. G. Weidler, E. Kaschka, G. Knoll, R. Nüesch, *Water Sci. Technol.* **2006**, *53*, 131–138.

[64] S. Komarneni, E. Breval, M. Miyake, R. Roy, *Clays Clay Miner.* **1987**, *35*, 385–390.

[65] S. Komarneni, R. Roy, D. M. Roy, *Cem. Concr. Res.* **1986**, *16*, 47–58.

[66] M. Tsuji, S. Komarneni, P. Malla, *J. Am. Ceram. Soc.* **1991**, *74*, 274–279.

[67] M. Diez-Garcia, J. J. Gaitero, J. S. Dolado, C. Aymonier, *Angew. Chem. Int. Ed Engl.* **2017**, *56*, 3162–3167.

[68] N. S. Bell, S. Venigalla, P. M. Gill, J. H. Adair, *J. Am. Ceram. Soc.* **1996**, *79*, 2175–2178.

[69] S. Merlino, E. Bonaccorsi, T. Armbruster, *Eur. J. Mineral.* **2001**, *13*, 577–590.

[70] K. Lin, J. Chang, J. Lu, *Mater. Lett.* **2006**, *60*, 3007–3010.

[71] S. A. S. El-Hemaly, T. Mitsuda, H. F. W. Taylor, *Cem. Concr. Res.* **1977**, *7*, 429–438.

[72] M. Sakiyama, T. Mitsuda, *Cem. Concr. Res.* **1977**, *7*, 681–685.

CONCEPT

This paper enlightens a fast and continuous method to synthesize phyllo- and inominerals. In few tens of seconds, highly crystalline and synthetic nanosized talc, synthetic xonotlite or synthetic tobermorite are produced using this process. This article highlights a new, efficient and sustainable route towards the development of new advanced and functional materials.

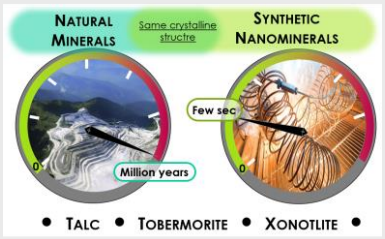

*Marie Claverie, Marta Diez-Garcia, François Martin and Cyril Aymonier **

Page No. – Page No.

Continuous synthesis of nanominerals in supercritical water